The ATHLET-MF Code and Its Application to Heavy Liquid Metal Cooled Systems

H. Y. Chen, X. Cheng
Institut für Kern- und Energietechnik
Programm Nukleare Sicherheitsforschung

Forschungszentrum Karlsruhe

in der Helmholtz-Gemeinschaft

Wissenschaftliche Berichte

FZKA 7165

The ATHLET-MF Code and Its Application to Heavy Liquid Metal Cooled Systems

H. Y. Chen, X. Cheng

Institut für Kern- und Energietechnik

Programm Nukleare Sicherheitsforschung

Abstract

This report presents a system thermal-hydraulic analysis code ATHLET-MF --- a new version of ATHLET. This code has been developed on the basis of ATHLET for the thermal-hydraulic analysis of multi-fluid systems, including the liquid LBE-cooled systems.

A fluid index was introduced in ATHLET-MF so that the user can easily adapt the code for various fluids. The current version of ATHLET-MF has the fluid options of water, liquid LBE and Diphyl THT. Empirical equations of physical properties of liquid LBE and of Diphyl THT, and the heat transfer correlation of liquid LBE were implemented in ATHLET-MF for its application to the LBE-cooled ADS systems. The physical properties and heat transfer correlation of liquid LBE were used based on the comprehensive review and assessment of the thermophysical properties of liquid LBE and of the heat transfer correlations for heat transfer in heavy liquid metals in the open literature.

The ATHLET-MF code was applied to the analyses of the target cooling systems of XADS, MEGAPIE and MITS under various transient conditions. The code was assessed against two home-made system analysis codes HERETA and HETRAF by performing the simulation of the dynamic behavior of the target cooling system of XADS under beam power switch-on conditions. Results from the three different codes show a good agreement, indicating the applicability of the ATHLET-MF code to LBE cooled systems.

Simulation of the beam power interruption of XADS shows that transient with longer beam interrupt time undergoes a deeper drop of the fluid temperature and of the mass flow rate. However, the drop of fluid temperature is limited by the heat transferred from the reactor pool and the reactor core after the switch-off of the beam power. It is shown that the beam interrupts with duration shorter than 0.1 s are less critical than those with duration longer than 0.1 s. In the case of loss of heat sink, the proton beam should be switched off in 200 s after the occurrence of the transient in order to avoid the failure of the window.

For the beam trips of MEGAPIE and MITS, a proper regulation of the 3-way valve in the intermediate cooling loop can effectively limit the LBE temperature fluctuation at the exit of the target heat exchanger. The peaks of LBE temperatures at the inlet and exit of the target heat exchanger after the beam power recovery can be reduced or even eliminated by opening the 3-way valve in the intermediate cooling loop at an early time. Comparison shows that the drop of fluid temperature under the transient of beam trip of MITS is much smaller than that of the MEGAPIE.

The steady state natural circulation of LBE is established after the loss of pump power supply for both MEGAPIE and MITS. The natural circulation flow rate is about 46% of its initial value for MEGAPIE and about 37% of its initial value for MITS, which is about 24% less than that calculated based on the proposed scaling principles of a scaled experiment.

ATHLET-MF:
Ein Rechenprogramm für das Kühlsystem mit flüssigen Schwermetallen

Kurzfassung

Im Rahmen der Entwicklung eines beschleunigergetriebenen unterkritischen Systems (ADS) zur Transmutation von radioaktiven Abfällen wurde das Programm ATHLET-MF zur Analyse des thermohydraulischen Verhaltens von Kühlsystemen entwickelt. Die Entwicklung basiert auf dem Programm ATHLET, das von der Gesellschaft für Reaktorsicherheit (GRS) für die transiente Analyse des wassergekühlten Reaktorkühlsystems entwickelt wurde.

Das Programm ATHLET-MF kann auf Kühlsysteme mit unterschiedlichen Fluiden angewandt werden. Die neue Version des Programms enthält die Anwendungsmöglichkeit für Wasser, Blei-Wismut und Diphyl THT. Die Struktur des Programms ist so gestaltet, dass die Benutzer das Programm leicht auf andere Fluide erweitern können. Der Vorgang der Erweiterung des Programms auf ein neues Fluid, z.B. Blei-Wismut, wird in diesem Bericht beschrieben. Die Stoffdaten und einige physikalische Modelle werden nach ihrer Genauigkeit evaluiert und ins Programm implementiert.

Systematische Untersuchungen zum thermohydraulischen Verhalten des Kühlsystems verschiedener Blei-Wismut-gekühlter Spallationstargets, nämlich XADS, MEGAPIE und MITS, wurden mit dem ATHLET-MF Programm durchgeführt. Der Vergleich der Ergebnisse aus dem ATHLET-MF Programm mit denen aus zwei weiteren System-Programmen zeigt eindeutig die Anwendbarkeit des Programms ATHLET-MF auf Blei/Wismut-gekühlte Systeme. Außerdem geben die Ergebnisse grundlegende Kenntnisse über das dynamische Verhalten der Kühlsysteme, Hinweise für die Auslegung erforderlicher Sicherheitsmaßnahmen und verbesserte Interpretation des Out-of-Pile Experiments MITS.

CONTENTS

1 INTRODUCTION

The accelerator driven subcritical reactor system (ADS) is a coupling system of a high energy proton accelerator and a subcritical reactor, offering a promising solution for reducing the amount of high-level radioactive waste to be disposed. It has raised significant interest and becomes a major R&D topic worldwide (DOE, 1999; ENEA, 2001; Mukaiyama, 1997).

In the design of an ADS, heavy liquid metals (HLM), such as lead bismuth eutectic (LBE), are considered as the reference coolant for both the subcritical reactor core and the spallation target due to its low melting point, efficient heat removal properties and high production rate of neutrons. The system analysis is required for the thermal-hydraulic design of both the reactor cooling system and the spallation target cooling system of ADS. Since many years, the Forschungszentrum Karlsruhe has involved in the design of different kinds of spallation targets (Cheng, 2000, 2002; Knebel, 2002). Two independent system analysis codes, HETRAF and HERETA, have been developed and applied to the design analysis of various spallation targets of ADS (Neitzel, 2002; Cheng, 2003).

Most recently, the system analysis code ATHLET-MF was developed for ADS application. This code is based on the ATHLET code, which was developed at the Gesellschaft für Reaktorsicherheit (GRS) and widely applied to water-cooled nuclear systems (GRS, 2001). Compared to ATHLET, the new developed ATHLET-MF code introduced fluid indexes to cope with the application to multi-fluid systems. The code structure was modified in such a way that the user can easily adapt the code for various fluids, e.g. liquid metals or supercritical pressure water.

For its application to LBE-cooled ADS, correlations of LBE thermophysical properties as well as heat transfer were selected and implemented in ATHLET-MF based on a comprehensive review and assessment of available studies in the open literature. Besides, thermophysical properties of Diphyl THT (DTHT) were also implemented into the code, which is considered as the secondary coolant of the LBE-cooled spallation target.

The new developed code ATHLET-MF was applied to the cooling system of the European Experimental ADS (XADS) (Cinotti, 2001a; Richard, 2002), and the heat removal system (HRS) of MEGAwatt PIlot target Experiment (MEGAPIE) (Bauer, 2001) and of the MEGAPIE Integral Test Stand (MITS). Analyses were performed for the steady state operation and various transient scenarios, e.g. beam power switch-on, loss of heat sink, beam power interruption and loss of pump power supply, to study the thermal-hydraulic behavior of the target cooling system.

In this report, modifications of the ATHLET code are introduced. The simulations of various transients of the cooling systems of the XADS target, the MEGAPIE and MITS using ATHLET-MF are presented. Results of the ATHLET-MF are compared with those of the HERETA and HETRAF.

2 THE ATHLET-MF CODE

2.1 Main Features

The ATHLET-MF code is a multi-fluid system analysis code modified from ATHLET (Analysis of Thermal-Hydraulics of LEaks and Transients) (GRS, 2001), which was developed by the Gesellschaft für Reaktorsicherheit (GRS) for the analysis of anticipated and abnormal plant transients, small and intermediate leaks as well as large breaks in light water reactors. The main features of ATHLET-MF are:

- Modular code architecture

- Simulations of transient, 1-dimensional, incompressible fluids with volumetric heat source

- Multi-fluid systems with thermal coupling

- Separation between physical models and numerical methods

- Simulation of control and balance of systems

- Pre- and post-processing tools

2.2 Code Structure

The ATHLET-MF code has the same structure as the ATHLET code. As shown in Figure 1, it composes of the basic modules of Thermo-Fluiddynamics (TFD), Heat Conduction and Heat Transfer (HECU), Neutron Kinetics (NEUKIN), General Control Simulation Module (GCSM) and Numerical integration method (FEBE) for simulating different phenomena involved in the operation of nuclear reactor systems. Detailed introduction about the basic models is given in (GRS, 2001).
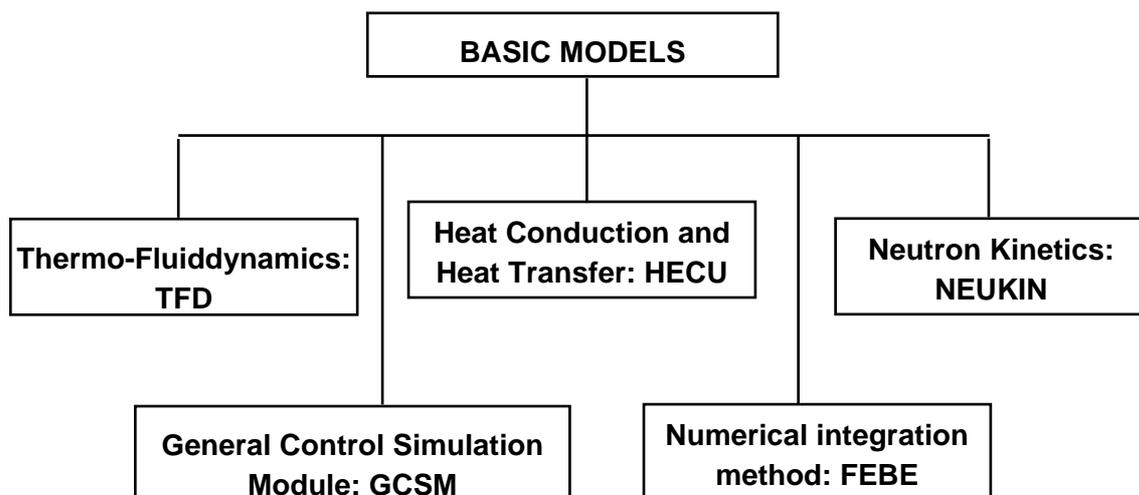
Figure 1 The basic models of ATHLET-MF

The ATHLET-MF code consists of about 800 subroutines with total size of 6.9MB for the processing of:

- Control and organization module (ID letter: A) (ID letter: the first letter or the first two letters of a subroutine's name)

    . input (ID letter: AI)

    . output (ID letter: AO)

    . parallel processing (ID letter: AP)

- Modules:

    . Thermo-Fluiddynamics: TFD (ID letter: D)

    . Heat conduction and heat transfer: HECU (ID letter: H)

    . Neutron Kinetics: NEUKIN (ID letter: N)

    . Numerical integration method: FEBE (ID letter: F)

    . General Control Simulation Module: GCSM (ID letter: G)

- Component modes (ID letter: K)

    . pump mode (ID letter: KP)

    . separator mode (ID letter: KS)

    . valve mode (ID letter: KV)

- Physical modes (ID letter: M)

    . critical flow (ID letter: MC)

    . correlations for drift, slip, relative velocities (ID letter: MD)

    . pressure drop (friction) correlations (ID letter: MF)

    . interphacial mass and energy exchange models (ID letter: MG)

    . heat transfer models (ID letter: MH)

    . properties (ID letter: MP)

    . Critical discharge rate model: CDR1D (ID letter: M1)

- Service program for general use (ID letter: S) and for output (ID letter: SO)

Refer to (GRS, 2001) for more information about the code structure and the flow chart diagram of ATHLET.

2.3 Fluid identification

Compared with the ATHLET code, modifications were made of the control and organization module, the modules of TFD and HEC, and physical modes of heat transfer and properties in the ATHLET-MF code. The code structure was modified in such a way that the user can easily adapt the ATHLET-MF code for various fluids.

For the simulation of multi-fluid systems, the following fluid indexes were defined and introduced into ATHLET-MF:

IFL0 – Fluid index of priority chain

IFLO – Fluid index of thermo-fluid object K

IFLV – Fluid index of control volume I

The IFL0 is a user defined parameter and is input for each priority chain. The IFLO and IFLV were introduced for use in the processing of TFO model and HECU model, respectively. The array of IFLO is allocated by the subroutine **ALLOCDNW** and its dimension is defined in the module **CANW.** The array of IFLV is allocated by **ALLOCANW** and its dimension is defined in **CDNW**. The IFLO for each thermo-fluid object is specified when the topology data are read by the subroutine **AITOP**, and the IFLV for each control volume of a priority chain is specified when the object specific network data are read by the subroutine **DINETW.**

ATHLET-MF has no limitation on the number of independent hydrodynamic systems to be simulated. With the introduction of above mentioned fluid indexes, thermophysical properties and physical models of various fluids can easily be implemented into the new developed ATHLET-MF code.

For the current ATHLET-MF version the options for IFL0, IFLO and IFLV are:

IFL0, IFLO, IFLV = 1: Water

IFL0, IFLO, IFLV = 2: Liquid Lead-Bismuth Eutectic

IFL0, IFLO, IFLV = 3: Diphyl THT

2.4 Thermo-physical Properties

2.4.1 Assessment of thermophysical properties

In the open literature, data and correlations of thermo-physical properties of LBE are found in numerous references. Data on the thermophysical properties of LBE were reported in the following references:

- Lyon (1952) for density, heat capacity, dynamic viscosity, thermal conductivity, surface tension

- Kutateladze et al. (1959) for density, heat capacity, dynamic viscosity, thermal conductivity

- MacLain and Martens (1964) for density, heat capacity, dynamic viscosity, thermal conductivity

- Holman (1968) for density, heat capacity, dynamic viscosity, thermal conductivity

- Hultgren et al. (1973) for heat capacity

- Kaplun et al. (1979) for dynamic viscosity

- Iida and Guthrie (1988) for thermal conductivity

- Alchagirov et al. (2003) for density

Table 1 lists the temperature range, number of data, and composition in weight percent of the available data on the thermophysical properties of LBE.

Kaplun et al. (1979) fit their own viscosity data to the following equation in the temperature range from 125 ^{o}C to 907 ^{o}C:

$$\mu = 4.656 \times 10^{-4} \exp\left(\frac{773.2}{T}\right) \tag{1}$$

where μ is the dynamic viscosity in kg/(m·s) and T is the temperature in K.

Alchagirov et al. (2003) correlated their own density data by the following empirical equation in temperature range from 137 ^{o}C to 453 ^{o}C:

$$\rho = 10981 - 1.137T \tag{2}$$

where ρ is the density in kg/m^3 and T is the temperature in K.

Figure 2, Figure 3 and Figure 4 compare the reported data of density, dynamic viscosity and thermal conductivity of LBE. It is shown that the data of both the density and the dy-

namic viscosity reported by different authors show a good agreement. However, the data of thermal conductivity reported by Kutateladze et al. (1959) are obviously higher than the data reported by Lyon (1952) which show a good agreement with the data reported by MacLain and Martens (1964). The data of thermal conductivity given by Iida and Guthrie (1988) lie between the data of Kutateladze et al. (1959) and the data of Lyon (1952). For lower temperature the thermal conductivity data of Iida and Guthrie (1988) agree with those of Lyon (1952), and for higher temperature agree with those of Kutateladze et al. (1959). By best fitting the data of Lyon (1952), the data of Kutateladze et al. (1959), the data of MacLain and Martens (1964), and the data of Iida and Guthrie (1988), one obtains,

$$\lambda = 4.4556 + 0.0128T \tag{3}$$

where λ is the conductivity in W/(m.°C) and T is the temperature in K.

Lyon reported a constant value of 146.4 J/(kg.K) for the heat capacity of LBE in the temperature range of 144 °C to 358 °C. The same value was reported by Kutateladze et al. (1959), MacLain and Martens (1964) and Holman (1968). Hultgren (1973) reported a linear decrease in heat capacity with temperature from melting point to 1000 K and recommended the following empirical equation,

$$C_p = 160.0 - 2.385 \times 10^{-2} T \tag{4}$$

where C_p is the heat capacity in J/(kg·K) and T is the temperature in K.

For the surface tension of LBE, the only data found in the literature were two values reported by Lyon (1952), i.e. 0.367 N/m at 800 °C and 0.356 N/m at 1000 °C. The values were correlated by Davis and Shieh (2000) with the following equation for use in the ATHENA code:

$$\sigma = 0.367 - 5.55 \times 10^{-5} \times (T - 1073.15) \tag{5}$$

where σ is the surface tension in N/m and T is the temperature in K.

Cevolani (1998) compared the LBE thermophysical property data reported by Lyon (1952), Kutateladze et al. (1959), MacLain and Martens (1964), Holman (1968), and, based mainly on the data of Lyon (1952), recommended a reference correlation as a function of temperature for each property of LBE. The correlations suggested by Cevolani (1998) have been programmed for use in thermal-hydraulic codes in ANSALDO. See Table 2 for the correlations proposed by Cevolani.

Imbeni et al. (1999) recommended another set of empirical equations (see Table 2) for the properties of LBE based on the data of Lyon (1952), Kutateladze et al. (1959), MacLain and Martens (1964), Hultgren (1973), Iida and Guthrie (1988), and the equations given by Cevolani (1998). The equation of density recommended by Imbeni et al. (1999) is the same as the one suggested by Cevolani (1998). However, the equation of heat capacity recommended by Imbeni et al. (1999) is based on the linear regression of the data reported by Hultgren et al. (1973), i.e. Eq. (4), and the equation of viscosity is obtained by fitting the data

reported by MacLain & Martens (1964), and the equation of thermal conductivity is obtained by linear regression of the values given by Kutateladze et al. (1959), which was also recommended for use in SIMMER-III (Morita et al., 2004).

Sobolev (2002) compiled a database of the LBE properties (see Table 2) for MYRRHA design calculation based mainly on the data of Lyon (1952), Kutateladze et al. (1959), MacLain and Martens (1964), Holman (1968), Hultgren (1973), Kaplun et al. (1979), and the application of the additivity rule of mixing (Raoult's law) to determine the density and viscosity, and the application of Wiedemann-Franz-Lorenz law to determine the thermal conductivity.

Table 1: Pb-Bi thermophysical property data from literature

| Property	Author	Temperature, ºC	No. of points	Composition, wt%
Density	Lyon (1952)	200 - 1000	5	44.5%Pb-55.5%Bi
	Kutateladze et al. (1959)	130 - 700	13	44.5%Pb-55.5%Bi
	MacLain and Martens (1964)	204 - 760	6	44.5%Pb-55.5%Bi
	Holman (1968)	288 - 649	2	44.5%Pb-55.5%Bi
	Alchagirov et al. (2003)	137 - 453	84	44.5%Pb-55.5%Bi
Dynamic vis-cosity	Lyon (1952)	332 - 600	5	44.5%Pb-55.5%Bi
	Kutateladze et al. (1959)	130 - 700	13	44.5%Pb-55.5%Bi
	MacLain and Martens (1964)	204 - 760	5	44.5%Pb-55.5%Bi
	Holman (1968)	288 - 649	2	44.5%Pb-55.5%Bi
	Kaplun et al. (1979)	394 -1180	275	44.5%Pb-55.5%Bi
Heat capacity	Lyon (1952)	144 - 358	1	44.5%Pb-55.5%Bi
	Kutateladze et al. (1959)	130 - 700	1	44.5%Pb-55.5%Bi
	MacLain and Martens (1964)	315.6 – 426.7	1	44.5%Pb-55.5%Bi
	Holman (1968)	288	1	44.5%Pb-55.5%Bi
	Hultgren (1973)	124 - 700	10	44.5%Pb-55.5%Bi
Thermal con-ductivity	Lyon (1952)	160 - 320	5	44.5%Pb-55.5%Bi
	Kutateladze et al. (1959)	130 - 700	13	44.5%Pb-55.5%Bi
	MacLain and Martens (1964)	204.4 - 426.7	3	44.5%Pb-55.5%Bi
	Iida & Guthrie (1988)	150 - 500	8	44.5%Pb-55.5%Bi
surface tension	Lyon (1952)	800 - 1000	2	44.5%Pb-55.5%Bi
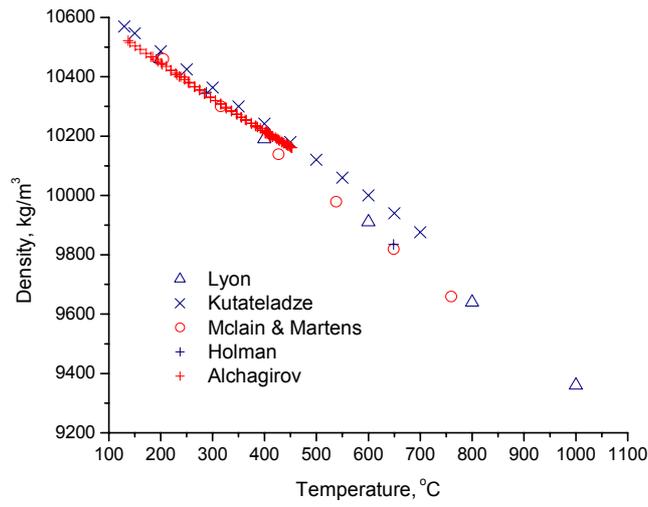
Figure 2 Density of LBE as function of temperature
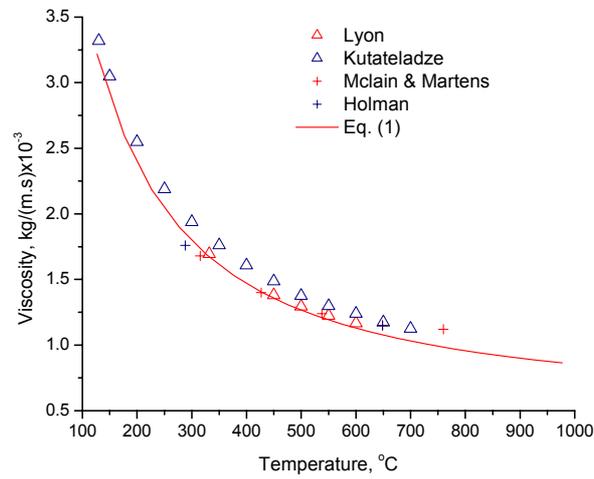
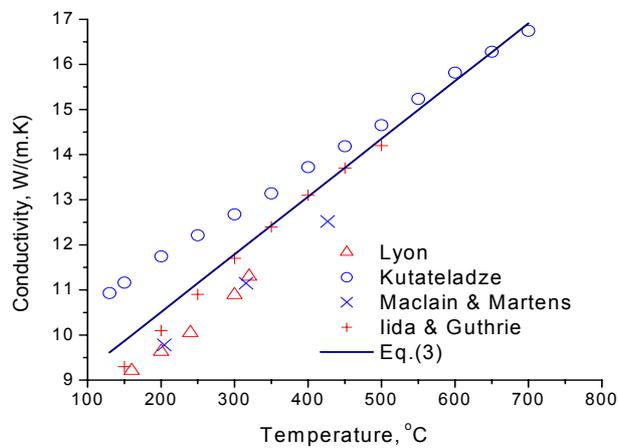Figure 3 Viscosity of LBE as function of temperature

Figure 4 Conductivity of LBE as function of temperature

9

Table 2: Correlations of liquid Pb-Bi thermophysical properties (temperature in K)

Author	Property	Unit	Correlations	Data base applied
Cevolani (1998)	Density	kg/m^3	$\rho = 11112 - 1.375T$	Lyon (1952)
	Dynamic viscosity	kg/(m.s)	$\mu = 5.37 \times 10^{-3} - 8.29 \times 10^{-6}T + 4.71 \times 10^{-9}T^2$	Lyon (1952)
	Heat capacity	J/(kg.K)	146.5	Lyon (1952)
	Thermal conductivity	W/(m.K)	$\lambda = 3.90 + 0.0123T$	McLain (1964)
Imbeni et al. (1999)	Density	kg/m^3	$\rho = 11112 - 1.375T$	Lyon (1952)
	Dynamic viscosity	kg/(m.s)	$\mu = 4.97 \times 10^{-4} \exp\left(\dfrac{741}{T}\right)$	McLain (1964)
	Heat capacity	J/(kg.K)	Eq. (4)	Hultgren (1973)
	Thermal conductivity	W/(m.K)	$\lambda = 6.851 + 0.0102T$	Kutateladze (1959)
Sobolev (2002)	Density	kg/m^3	$\rho = 11102 - 1.321T$	Lyon (1952), Kutateladze (1959), Vegard's superposition law (VSL)
	Dynamic viscosity	kg/(m.s)	$\mu = 4.94 \times 10^{-4} \exp\left(\dfrac{754}{T}\right)$	Kutateladze (1959), Lyon (1952), McLain (1964), Holman (1968), Kaplun (1979)
	Heat capacity	J/(kg.K)	$C_p = 164.0 - 4.06 \times 10^{-2}T + 1.33 \times 10^{-5}T^2$	Hultgren (1973), VSL
	Thermal conductivity	W/(m.K)	$\lambda = 3.35 + 1.59 \times 10^{-2}T - 1.95 \times 10^{-6}T^2$	Kutateladze (1959), Lyon (1952), McLain (1964), Iida (1988), Wiedemann-Franz-Lorenz law
Petrazzini (2002)	Dynamic viscosity	kg/(m.s)	$\mu = 0.843 \times 10^{-3} \times \left(1.17 \times \exp(\dfrac{1006.5}{T} - 1.68) + 0.90 \times \exp(\dfrac{670.8}{T} - 1.23)\right) + 0.12 \times 10^{-3}$	Lyon (1952), Iida (1988), Buono (1997)
	Thermal conductivity	W/(m.^{o}C)	$\lambda = \dfrac{2.45T}{0.075T + 77.525}$	Lyon (1952), Iida (1988), Buono (1997)
	Surface tension	N/m	$\sigma = 0.3754 - 9.66 \times 10^{-5} \times (T - 973.15)$	Lyon (1952), Iida (1988), Buono (1997)

Petrazzini (2002) reported a set of LBE physical properties and thermodynamic tables for the LBE cooled ADS studies on the basis of different sources of data on lead, bismuth and lead-bismuth eutectic (Lyon, 1952; Iida and Guthrie, 1988; Buono, 1997). In his report, the physical properties of liquid thermal conductivity, dynamic viscosity and surface tension were fitted by means of mathematical correlations as a function of temperature. The tables of density and heat capacity of LBE were generated using the soft-sphere model (Young, 1977) for 52 points of temperature and 19 points of pressure.

The International Nuclear Safety Center at Argonne National laboratory (INSC) recommends the following equation for the viscosity of LBE from the melting point 125 $^{\circ}$C to 1000 $^{\circ}$C,

$$\mu = 4.90 \times 10^{-4} \exp\left(\frac{760.1}{T}\right) \tag{6}$$

where μ is the dynamic viscosity in kg/(m·s) and T is the temperature in K. This equation was obtained by fitting the data of Kaplun et al. (1979), Kutateladze et al. (1959), and Bienas and Sauerward (1927). This equation was proposed for use in SIMMER-III (Morita et al., 2004).

Based on the empirical equations of surface tension for liquid lead and bismuth (Al-chagirov and Mozgovoi, 2003) and the additivity rule of mixing, Morita et al. (2004) proposed the following equation for the surface tension of LBE:

$$\sigma = 0.4537 \times \left(1 - \frac{T}{4890}\right)^{0.8640} \tag{7}$$

where σ is the surface tension N/m and T is the temperature in K.

For the thermal expansion, the only empirical equation was recommended by Sobolev (2002):

$$\beta = \frac{1}{8404 - T} \tag{8}$$

where β is the thermal expension in 1/K and T is the temperature in K. This equation was obtained simply by the substitution of the density equation (Sobolev, 2002) into the equation defining the coefficient of volumetric thermal expansion, i.e.,

$$\beta(T) = -\frac{1}{\rho} \cdot \frac{\partial \rho}{\partial T} \tag{9}$$

where ρ is the density in kg/m^3 and T is the temperature in K.

Table 2 summarizes the available empirical correlations for the thermophysical properties of LBE.

Figure 5 compares the density equations of LBE recommended by different authors. It is shown that the density equations of LBE show a good agreement for the temperature lower than 600 °C. The differences of density between different equations increase with increasing temperature. At 800 °C the difference of density (the biggest) between the equation of Cevolani and equation of Alchagirov is ~12.6%; and at 1000 °C the difference of the two equations is ~ 18%. Since the density equation of Cevolani was obtained by fitting the data of Lyon (1952), which cover a temperature range up to 1000 °C, this equation was proposed for use in ATHLET-MF.

The equations of dynamic viscosity show a good agreement with the only exception of the equation of Cevolani for temperature lower than 300 °C, see Figure 6. Equation (1) was obtained by fitting the data of Kaplun, which consist of total 275 measurement points in the temperature range from 120 °C to 906 °C. This equation was therefore recommended for use in ATHLET-MF.

Comparison of thermal conductivity equations is shown in Figure 7. The discrepancies among the equations are expected due to the factor of different data sources on which equations are based. The equation of Sobolev (2002) agrees with Equation (3) since they are based on the same data sources. It was recommended that Equation (3) be used in ATHLET-MF.

Figure 8 compares the available two equations for the heat capacity of LBE: the Equation (4) and the equation obtained by Sobolev (2002). It is seen that the two equations show a good agreement. It was proposed that Equation (4) be used in ATHLET-MF.

The surface tension equations of LBE are compared in Figure 9. The equations show good agreement, especially for higher temperature. Equation (5) was obtained based on the data of Lyon (1952) and was proposed to be used in ATHLET-MF.

Data and equations of thermophysical properties of vapor LBE and DTHT were hardly to be found in the literature, and therefore the current version of ATHLET-MF is limited only to the application of single liquid phase of LBE and of DTHT.

As a summary, Table 3 lists all the equations of thermophysical properties of LBE which were proposed to be used in ATHLET-MF in the temperature range from 130 °C to 800 °C.

It is seen from above discussion that the measurement of LBE thermal conductivity at low temperature and the measurement of LBE heat capacity would be of interest in the future.
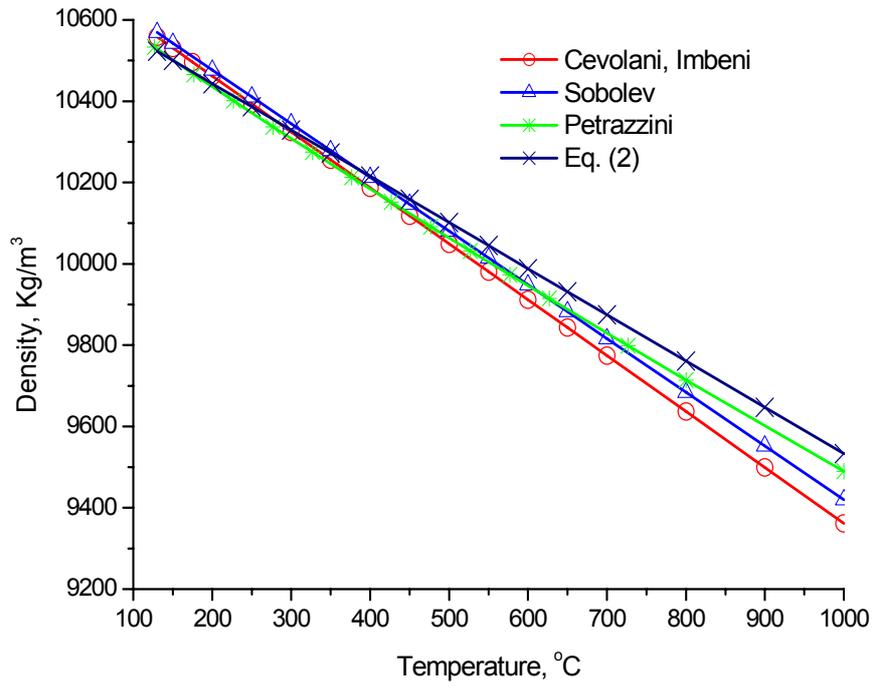
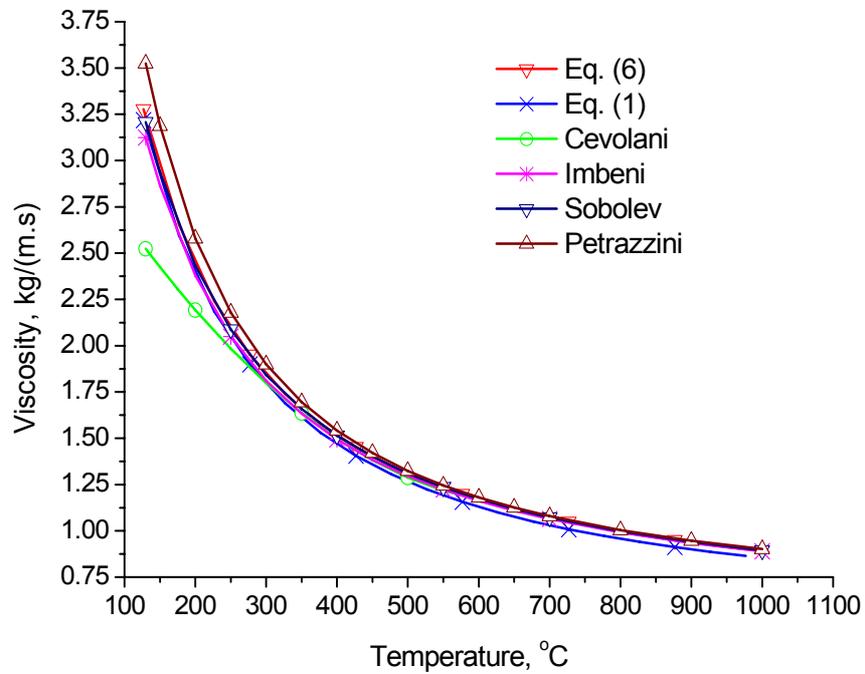Figure 5 Comparison of LBE density equations

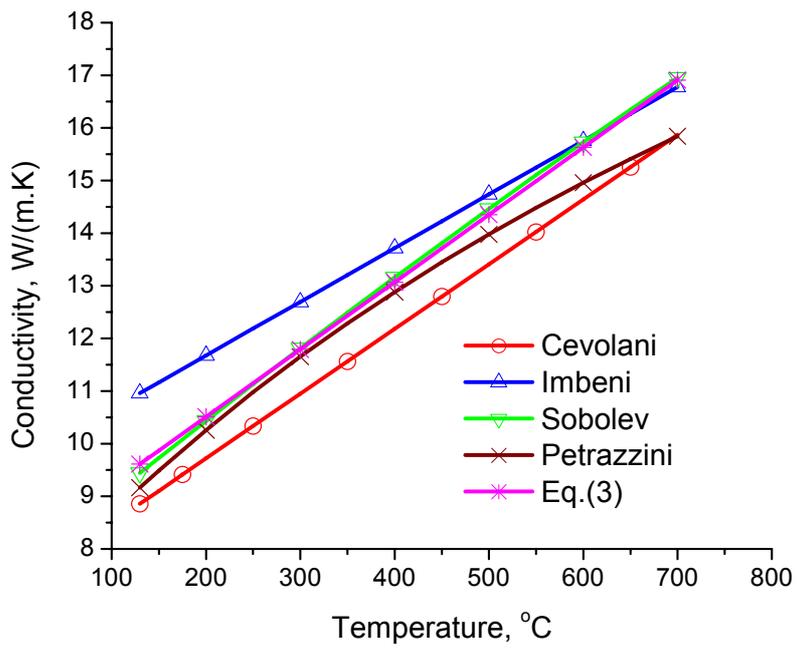Figure 6 Comparison of LBE dynamic viscosity equations

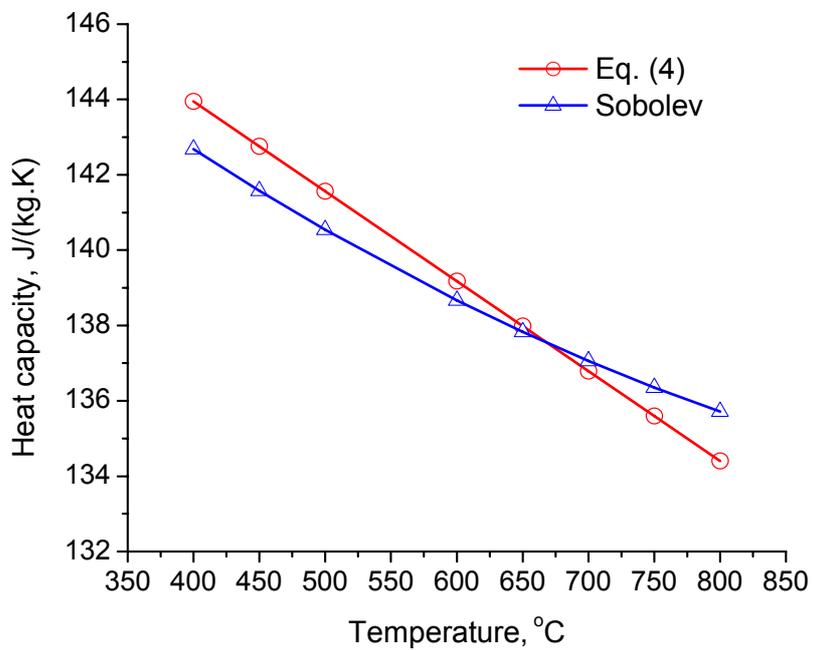Figure 7 Comparison of LBE thermal conductivity equations

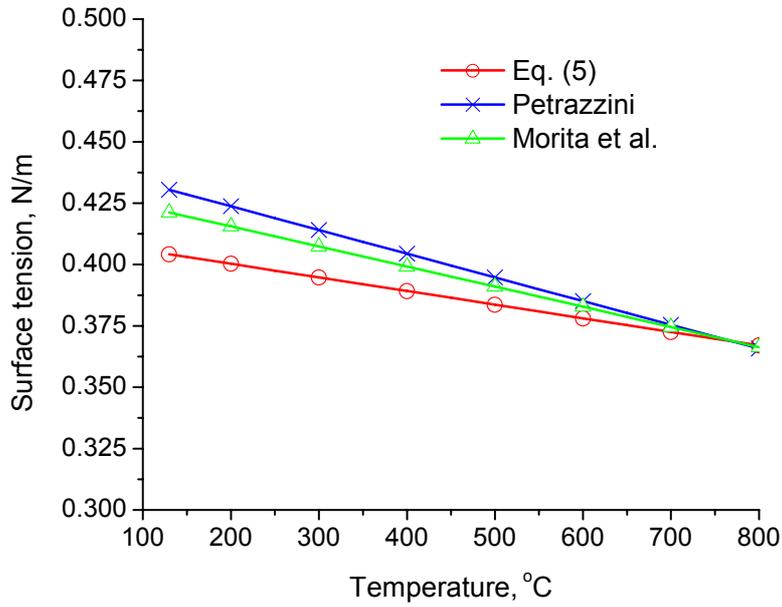Figure 8 Comparison of LBE heat capacity equations

14

Figure 9 Comparison of LBE surface tension equations

Table 3: Equations of Physical properties of LBE used in ATHLET-MF*

Property	Unit	Correlation
Density	kg/m^3	$\rho = 11112 - 1.375T$
Thermal conductivity	W/(m.K)	$\lambda = 4.4556 + 0.0128T$
Specific heat	J/(kg.K)	$C_p = 160.0 - 2.385 \times 10^{-2}T$
Dynamic viscosity	kg/(m·s)	$\mu = 4.656 \times 10^{-4} \exp\left(\dfrac{773.2}{T}\right)$
Surface tension	N/m	$\sigma = 0.367 - 5.55 \times 10^{-5} \times (T - 1073.15)$
Thermal expansion coefficient	1/K	$\beta = \dfrac{1}{8404 - T}$

* The unit of temperature in the table is K.

2.4.2 Implementation of thermophysical properties

The introduction of fluid indexes makes it convenient to implement thermophysical properties of various fluids in ATHLET-MF. For both XADS and MEGAPIE, the LBE is used as the coolant of the target system and the DTHT as the working fluid of the intermediate cooling loop, and therefore the thermophysical properties of LBE and of DTHT were implemented in the present version of ATHLET-MF. Due to the lack of the vapor properties of LBE and of DTHT, only the properties of the liquid LBE and of the liquid DTHT were implemented in the code. For both LBE and DTHT, the pressure has a negligible effect on the thermophysical properties, and therefore was not taken into account in the functions of the thermophysical properties of LBE and DTHT which were implemented in ATHLET-MF.

As listed in Table 3, the thermophysical properties of LBE are used in ATHLET-MF in the form of functions of temperature ranging from 130 ºC to 800 ºC, including the liquid density, thermal conductivity, dynamic viscosity, specific heat, surface tension, and thermal expansion coefficient.

The physical properties of DTHT were obtained from the manufacturer Bayer in the form of thermodynamic table (Neitzel, 2003). The data were correlated by the authors with equations as functions of temperature in the range from 20 ºC to 400 ºC, see Table 4.

Table 4: Physical properties of DTHT*

Property	Unit	Correlation
Density	kg/m^3	$\rho = 1013.5 - 0.645T$
Thermal conductivity	W/(m.K)	$\lambda = 0.1101 - 2.769 \times 10^{-5}T$
Specific heat	J/(kg.K)	$c_p = 1451.5 + 3.52T$
Dynamic viscosity	kg/(m·s)	$\mu = (48.5 Exp^{-T/28.2} + 4.223 Exp^{-T/95.8} + 0.241) \times 10^{-3}$
Surface tension	N/m	$\sigma = 0.0462 - 1.451 \times 10^{-4}T + 9.22 \times 10^{-8}T^2$

* The unit of temperature in the table is ºC.

For the transient simulation, the derivatives of properties as functions of temperature (*T*) are deduced based on the correlations listed in Tables 3 and 4. The liquid enthalpy (*h*) is calculated based on the equation $h = \int c_p dT$, where c_p is the specific heat and *T* the liquid temperature.

For the calculation of thermophysical properties of liquid LBE, the following subroutines were implemented in ATHLET-MF,

MPAROLM: density as function of enthalpy

MPHPTLM: enthalpy for given liquid temperature

MPPHPTM: enthalpy, specific volume and its derivatives for given temperature

MPPTM: enthalpy, specific volume and their derivatives at given temperature

MPTAFM: liquid properties (specific volume, specific enthalpy, thermal expansion num-
ber, specific heat capacity, surface tension, dynamic viscosity) at given
temperature

MPZUS1M: liquid properties (dynamic viscosity, specific heat capacity, thermal conduc-
tivity) at given temperature

MPZUS2M: properties (specific enthalpy, specific volume) and their derivatives for liquid
dominant equation system

And for DTHT, the following subroutines were implemented,

MPAROLO: density as function of enthalpy

MPHPTLO: enthalpy for given liquid temperature

MPPHPTO: enthalpy, specific volume and its derivatives for given temperature

MPPTO: enthalpy, specific volume and their derivatives at given temperature

MPTAFO: liquid properties (specific volume, specific enthalpy, specific heat capacity,
surface tension, dynamic viscosity) at given temperature

MPZUS1O: liquid properties (dynamic viscosity, specific heat capacity, thermal conductiv-
ity) at given temperature

MPZUS2O: properties (specific enthalpy, specific volume) and their derivatives for liquid
dominant equation system

In ATHLET-MF, subroutines for the calculation of thermodynamic properties are called
by those subroutines for processing thermo-fluiddynamic objects with the following com-
mends,

IF(IFLO(IOBJ).EQ.1) CALL SUBNAME

IF(IFLO(IOBJ).EQ.2) CALL SUBNAMEM

IF(IFLO(IOBJ).EQ.3) CALL SUBNAMEO

where

IOBJ   - Index of object in execution

SUBNAME – Subroutine of thermodynamic property of water

SUBNAMEM – Subroutine of thermodynamic property of LBE

SUBNAMEO – Subroutine of thermodynamic property of DTHT

The calling subroutines and the calling order for the subroutines of thermophysical
properties are shown in Figure 10.

Figure 10 Calling order of subroutines for the thermophysical properties in ATHLET-MF

18

2.5 LBE Heat Transfer Correlation

A heat transfer correlation for liquid LBE was implemented in ATHLET-MF. Since boiling of liquid LBE and of liquid DTHT is not expected at operational conditions of ADS, the convective heat transfers of liquid LBE and of liquid DTHT are simulated using single phase convective heat transfer correlations. The Dittus-Boelter correlation was applied for single phase convective heat transfer of DTHT.

For single phase convective heat transfer of LBE, Cheng et al. (2004) reviewed the available heat transfer correlations in the open literature for heat transfer in heavy liquid metals, especially liquid LBE. Based on their studies, the following correlation was proposed for heat transfer of LBE under conditions of uniform heat flux:

$$Nu = A + 0.018Pe^{0.8} \tag{12}$$

with

$$A = \begin{cases} 4.5 & Pe \leq 1000 \\ 5.4 - 9 \times 10^{-4} Pe & 1000 \leq Pe \leq 2000 \\ 3.6 & Pe \geq 2000 \end{cases} \tag{13}$$

where Nu is the Nusselt number and Pe is the Peclet number, which is a function of the Reynolds number and the Prandtl number ($Pe = Re \cdot Pr$). The characteristic length of the Reynolds number is the hydraulic diameter (D_h) of the flow channel.

The above heat transfer correlation was proposed for use in ATHLET-MF, and was implemented in the subroutines of MHTCN1, MHTCN2 and MHTCN3 by using the following comment,

IF(IFLV(ICV).EQ.2)HTC=(A+0.018*(RE*PR)**0.8)*(WLF/DHY)

where

ICV - index of control volume coupled to the heat conduction volume

HTC - heat transfer coefficient

A   - parameter defined by Eq. (10)

RE   - Reynolds number

PR   - Prandtl number of liquid LBE

WLF - thermal conductivity of liquid LBE

DHY - hydraulic diameter of coolant channel

In ATHLET-MF, subroutines for the calculations of thermodynamic properties are called by the subroutines for processing heat conduction objects with the following commends,

IF(IFLV(ICV).EQ.1) CALL SUBNAME

IF(IFLV(ICV).EQ.2) CALL SUBNAMEM

IF(IFLV(ICV).EQ.3) CALL SUBNAMEO

where

ICV   - Index of control volume coupled to the heat conduction volume

SUBNAME – Subroutine of thermodynamic property of water

SUBNAMEM – Subroutine of thermodynamic property of LBE

SUBNAMEO – Subroutine of thermodynamic property of DTHT

The calling subroutines are: **MHTCN1, MHTCN2, MHTCN3**.

The ATHLET-MF constitutive models for the calculations of wall friction and form losses are the same as those of ATHLET (Austregesilo, 2000).

3 CODE APPLICATION

The ATHLET-MF was applied to the analyses of various transients of the target heat removal systems of XADS, MEGAPIE and MITS. For the XADS, the beam power switch-on transient, beam power interruption and loss of heat sink were selected and simulated using the ATHLET-MF code. Two home-made system analysis codes HERETA and HETRAF were also used to simulate the beam power switch-on transient. Results of three codes were compared and the ATHLET-MF was assessed.

3.1 Analyses of transients for XADS target

3.1.1 The XADS target

The XADS is an 80 MW (th) European experimental ADS associated with a spallation neutron source, which will be constructed to study and to demonstrate the basic physical principles and practicability of ADS on an industrial scale. As shown in Figure 11, the LBE cooled XADS (Cinotti, 2001b) consists of mainly the spallation target, the sub-critical core, the primary loop and the secondary loop. It has two target design solutions: "window" target and "windowless" target. However, the "window" target solution will be the interest of the present study.
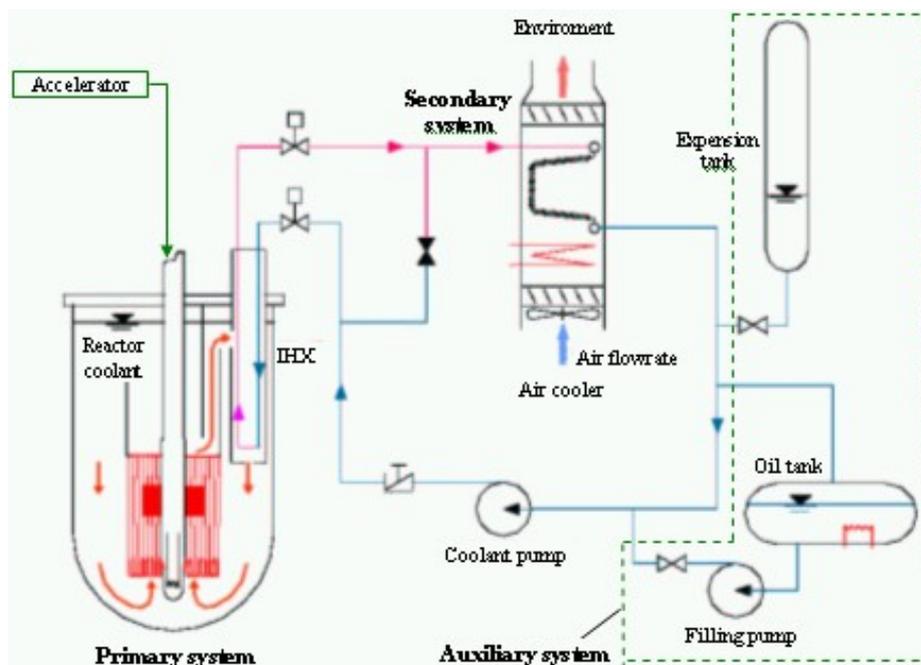

Figure 11   Sketch of the XADS reactor system with secondary loop
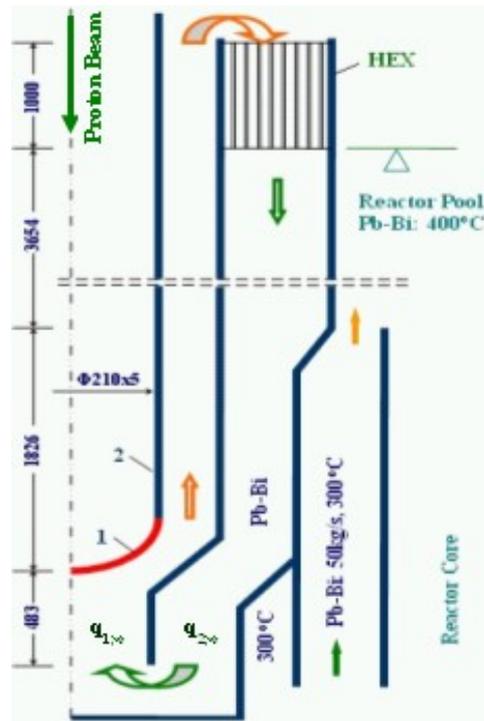and the auxiliary components

Figure 12 Schematic of XADS target system in a window configuration.
1- beam window; 2- beam tube. Diminsions in mm.

The LBE window target of XADS is schematically shown in Figure 12. It is a compact target module designed for a pool type reactor. The heat exchanger is integrated into the target unit, which make it possible to exchange the target without any change of the reactor. It consists of the central proton beam vacuum pipe and the inner and outer flow channels. The thin metallic window at the lower end of the beam tube acts as a physical separation of the flowing LBE from the vacuum space of the beam tube. The LBE flows upwards through the inner channel by natural convection as is heated up by the proton beam in the lower part of the target unit, centered at the core mid-plane. The coolant LBE is cooled down in the heat exchanger located in the upper part where the heat is transferred to the DTHT in the secondary side of the heat exchanger (HEX). A total heat of 2.62 MW is released in the spallation zone below the beam window, of which 80% is released in the inner channel and 20% in the outer channel. The diathermic fluid has the inlet temperature of about 170 °C and mass flow rate of 145 kg/s. The part of the target below the HEX is immersed in the LBE pool of the reactor with its top covered by gas. The average LBE temperatures of the reactor core and pool are 300 °C and 400 °C, respectively (Cinotti, 2001b).

3.1.2 Beam power transient

The dynamic behavior of the target cooling system under the beam power switch-on transient was analyzed by ATHLET-MF and two home-made system analysis codes HERETA and HETRAF. The HERETA code was developed specifically for the LBE cooled systems. It was applied to the design of the large-scale integral target test module K4T in KALLA (KArlsruhe Lead Laboratory) (Neitzel, 2002). The HETRAF code was originally developed for super-critical helium systems (Cheng, 1994). It was modified and extended to LBE systems. This code has been applied to the design analysis of the MEGAPIE (Knebel, 2001).

In this work, the beam power transient defined for the benchmark is assumed such that the heat exchanger is put into operation at the beginning of the transient and the beam power (2.62 MW) is switched on after 500 s. The beam power is assumed to be uniformly distributed in the spallation zone. The initial temperature of the whole target system is assumed to be 300 °C, and the initial mass flow rate is zero. For the whole transient, the LBE temperatures of the reactor core and the reactor pool are assumed to be 300 °C and 400 °C, respectively. For all the three codes, ATHLET-MF, HERETA and HETRAF, the same correlations of heat transfer, frictional pressure drop and LBE properties are employed.

Figure 13 compares the transient results, i.e. the LBE mass flow rate and temperature near the beam window, obtained using the three system analysis codes. After the transient begins, LBE is cooled down by the cooling oil of the secondary side of HEX. The LBE mass flow rate (see Figure 13a) increases due to the buoyant convection resulting from the difference of the fluid density between the inner channel and the outer channel. The mass flow rate reaches its peak before the cooled fluid enters the inner channel. Stable system mass flow rate and fluid temperature are achieved after the heat removal in HEX is balanced by the heat in-flow from the reactor pool to the outer channel. The mass flow rate and the fluid temperature show a sharp increase when the beam power is switched on. Another steady state condition with a higher mass flow rate and a higher fluid temperature is established at 700 s, about 200 s after the switch-on of the beam power.

Results from the three different codes show a good agreement. The present study clearly indicates the applicability of the ATHLET-MF code to LBE cooled systems.
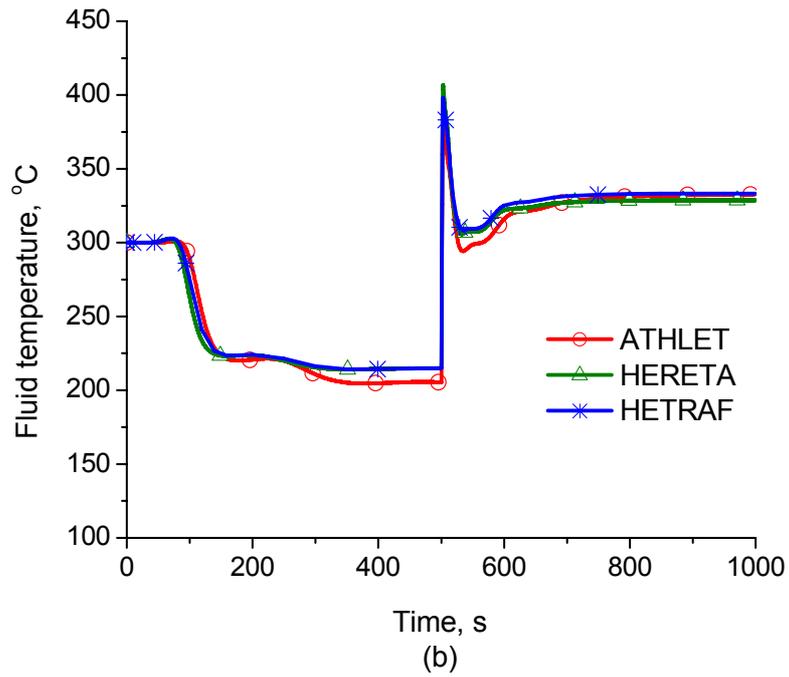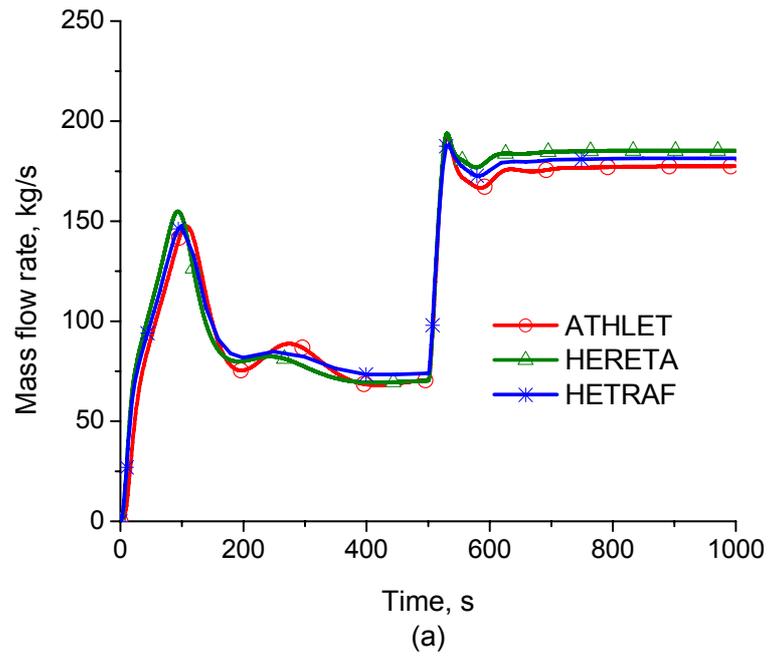
Figure 13 Comparison of results from different codes for the beam power transient
(a) mass flow rate; (b) fluid temperature below the beam window.

3.1.3 Beam power interruption and loss of heat sink

In the present study, the beam power interruption is defined under such conditions that the beam power is switched off from the full power operation status and is recovered again after 100 seconds, 30 seconds, 10 seconds and 3 seconds, respectively. The transient was simulated by the ATHLET-MF code.

Figure 14 shows the fluid temperature close to the beam window and the mass flow rate under the beam power interruption transient. Due to the sudden loss of the total heat source, the fluid temperature below the beam window drops sharply after the switch-off of the proton beam. The natural convection mass flow rate decreases due to the decrease of the buoyancy force resulting from the difference of the average fluid density between the outer flow channel and inner flow channel. The drop of mass flow rate depends on the beam inter-rupt time. The longer the beam interrupt time, the smaller the buoyancy force, and thus the deeper the drop of the mass flow rate. For the beam interrupt time greater than 30 seconds, a steady state natural convection with lower fluid temperature and mass flow rate is estab-lished after the switch-off of the beam power when the heat transferred from the reactor pool and the reactor core is balanced by the heat removed through the HEX. The fluid tempera-ture below the beam window shows an instant increase at the beam power recovery. It reaches its maximum in about 3 seconds and then decreases due to an increasing mass flow rate resulting from the increasing buoyancy force. After reaching its maximum, the mass flow rate decreases due to the decrease of the buoyancy force resulting from the decrease of the difference of the average fluid temperature between the outer channel and the inner channel. Transients with a longer beam interrupt time show a higher peak of fluid temperature and of mass flow rate after the beam power recovery. A steady state at full power operating condi-tion is re-established shortly after the beam power is recovered, in particular for the case with a shorter interrupt time.

Numerical simulation with CFX 5.6 for beam trips with interrupt durations less than 3 seconds shows the similar results (Tak et al., 2005). The CFX 5.6 simulation also shows that, regarding the peak temperature and temperature change rate, beam interrupts with duration shorter than 0.1 s are less critical than those with duration longer than 0.1 s. The interruption of beam power causes a large temperature fluctuation and hence should be avoided.

The fluid temperature and the mass flow rate under loss of heat sink (i.e. loss of secon-dary cooling fluid) are shown in Figure 15. The system is under steady state condition at the beginning, and the loss of secondary side cooling of HEX occurs at 200 s. Obviously, the fluid temperature of the target system increases after the loss of heat sink since only a limited part of heat is transferred from the target to the reactor pool. The mass flow rate, however, decreases sharply at the beginning due to the decrease of the buoyancy force. It tends to increase again after the temperature of the fluid coming from the outer channel reaches 400 °C and the heat is transferred from the outer channel to the reactor pool, and turns shortly to decrease when the difference of fluid density between the outer channel and the inner chan-nel continues to decrease. Based on the CFX simulation of XADS target (Tak et al., 2005), the maximum window surface temperature reaches its allowable temperature of 525 °C at about 400 s, i.e. 200 s after the transient occurs. It is concluded that the proton beam should be switched off in 200 s after the occurrence of loss of heat sink.
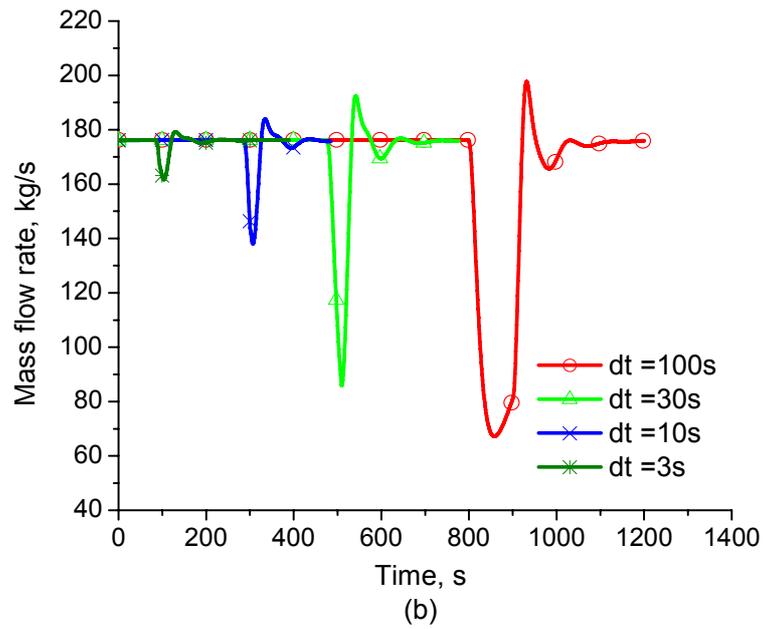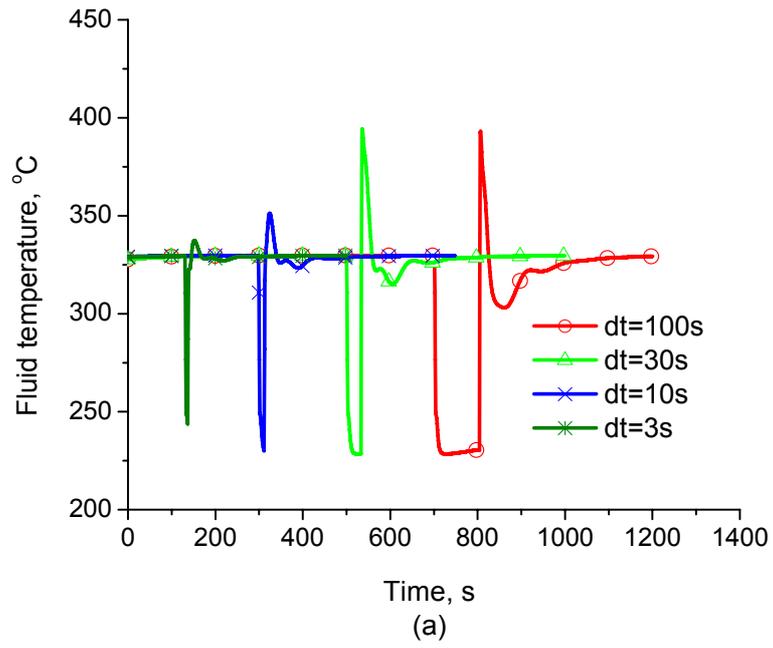
Figure 14 Variations of temperature (a) and mass flow rate (b)
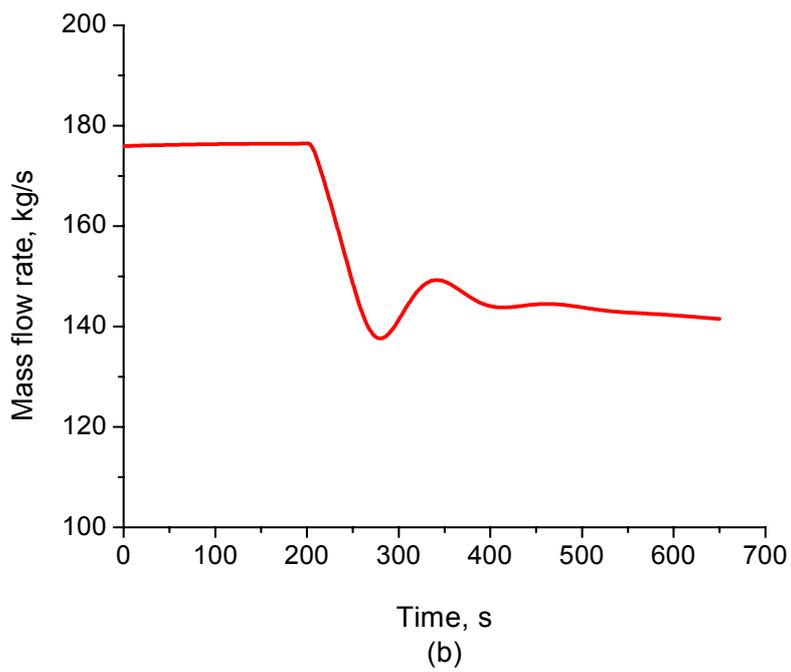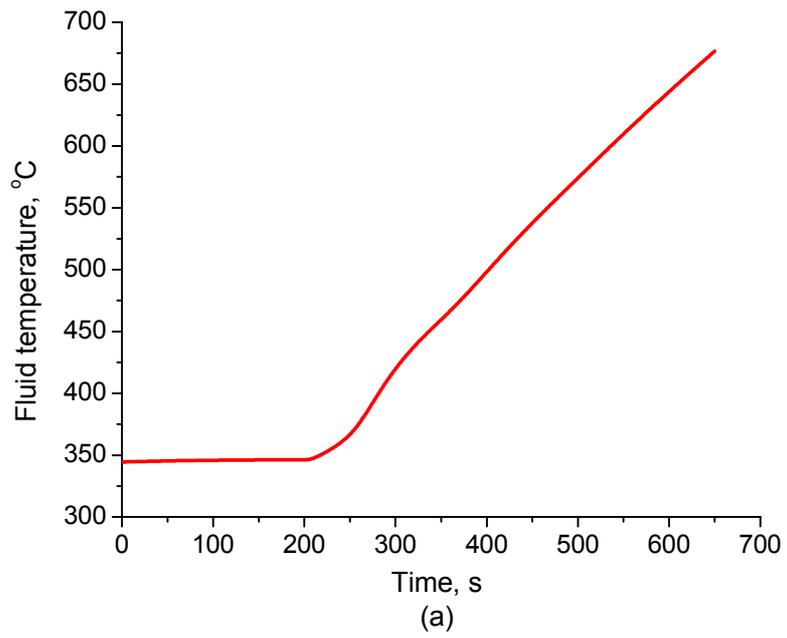for beam power interruption times

Figure 15 Variations of fluid temperature (a) and mass flow rate (b)
for a loss of the heat sink at t=200 s.

3.2 Analysis of the HRS of MEGAPIE and MITS

3.2.1 The MEGAPIE and MITS

The MEGAPIE project (Bauer, 2001) is a joint international research to design and to build a 1MW heavy liquid metal spallation neutron target, aiming at the demonstration of the technological feasibility of a liquid lead-bismuth target for a spallation neutron source and more important for the target technology of an ADS.

The MEGAPIE heat removal system (HRS), as shown schematically in Figure 16, consists of three loops, i.e. the primary LBE loop, the intermediate cooling loop (ICL) which has Diphyl THT (DTHT) as the working fluid, and the secondary water loop (SWL). The LBE target cooling loop, ICL and SWL are operated together to form the heat removal system.
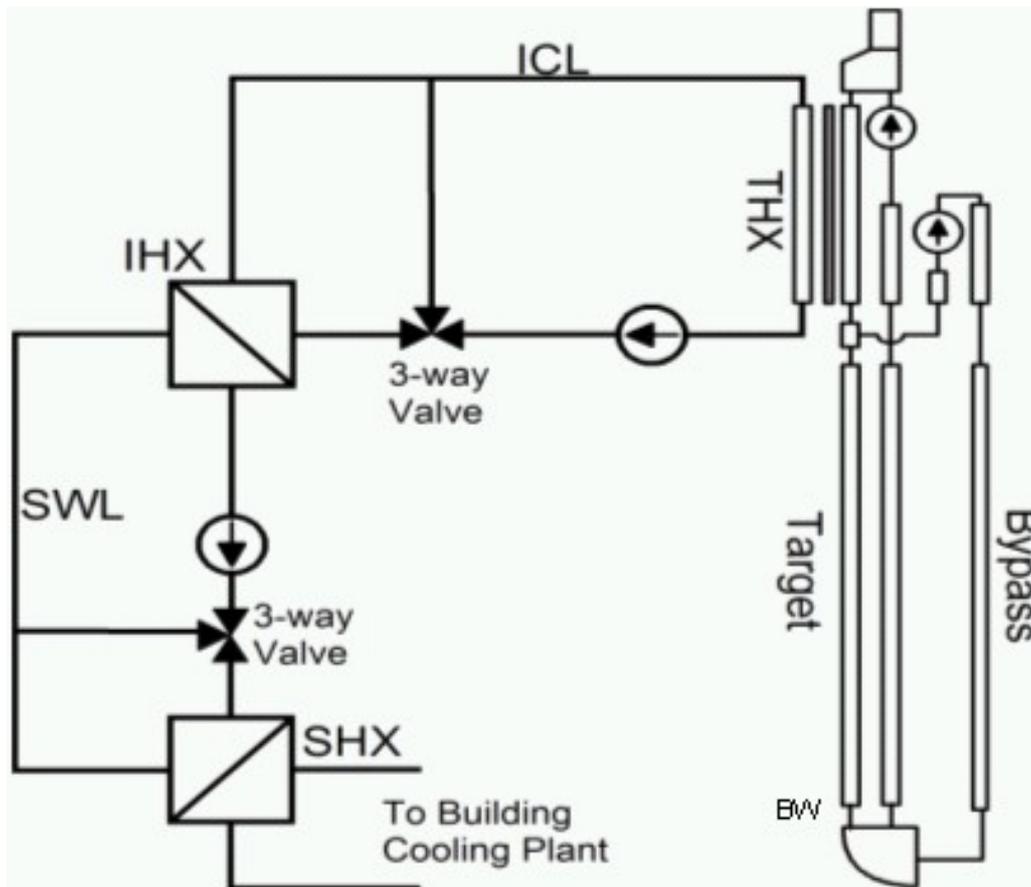

Figure 16 Schematic of MEGAPIE heat removal system

The LBE target cooling loop or the target itself, see Figure 17, is contained in a vertical liquid metal container (LMC) and can be divided into the upper part and the lower part. In the upper part of the target, there are one main electromagnetic pump (EMP) which circulates the main LBE coolant through the loop, one bypass EMP which drives a cooling jet toward the beam window (BW) in the lower part of the target, and a 12-pin target heat exchanger (THX) through which heat of the target is transferred to the ICL. The lower part of the target consists of the downcomer, beam window, central rod, and riser. The LBE coolant from the exit of main EMP turns around at the LBE expansion tank on the top of the target. It flows downwards through the THX. The downcomer guides the LBE flow from the exit of THX to the beam window. After passing the beam window, it turns upward into to the riser, and then to the inlet of the main EMP.
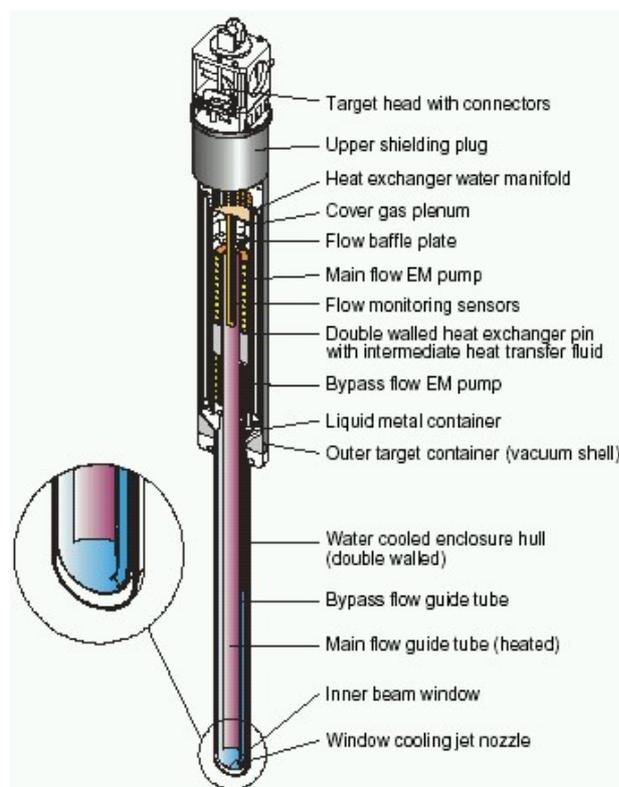

Figure 17 Schematic of the MEGAPIE target

ICL is a closed cooling loop that transports heat from the LBE coolant through the target heat exchanger (THX) in the upper target to SWL through the intermediate heat exchanger (IHX). It is filled with DTHT circulated by a centrifuge oil pump. A three-way control valve, installed upstream of IHX, distributes the flow between IHX and the bypass line during normal, part-load operation and during transients, in order to control the LBE cold leg temperature at a constant value. The SWL is almost like a copy of the ICL. It serves as a buffer between the ICL and the cooling plant of the building so that any possibility of DTHT leakage into the building cooling circuit is eliminated. This closed cooling water loop transports heat from the IHX to the secondary heat exchanger (SHX) where the building cooling circuit is connected to. A three-way valve is installed upstream of the SHX to regulate the bypass flow from the SHX so that the cold leg temperature can be stabilized at any transient conditions. For normal operation, the ICL is pressurized to 3.5 bar, and the SWL is pressurized to roughly 3 bar.

The MITS (MEGAPIE Integral Test Stand) is a full scaled MEGAPIE integral test facility for system integration and functional test of the MEGAPIE target system without proton beam heating. The proton beam heating is simulated by an electric heater of 200 kW attached to the bottom of the LMC. The flow rate and the temperature of MITS were scaled as (Leung, 2003):

$$\frac{m_s}{m_n} = \left(\frac{Q_s}{Q_n}\right)^{1/3}, \qquad and \qquad \frac{\Delta T_s}{\Delta T_n} = \left(\frac{Q_s}{Q_n}\right)^{2/3} \qquad respectively, \qquad (14)$$

where the subscripts n and s denote the nominal and scaled conditions, respectively.

The Eq. (14) was applied to the LBE loop of MITS. However, discrepancies are expected between the LBE loop of MEGAPIE and of MITS due to the deviation of simulation of the ICL and the SWL.

3.2.2 Transient of Protected Beam Trip

The proton beam trip is an important transient in the operation of MEGAPIE target because the proton beam suffers hundreds of trips in a week operation and roughly 10,000 trips during the target lifetime. In case of a beam trip, the MEGAPIE target, especially the beam window, must be protected from large temperature fluctuations in order to limit the risk of thermal ratcheting and thermal fatigue damage on the structure material. One of the solutions is to maintain a constant LBE temperature at the THX exit at any thermal transient conditions by regulating the 3-way valve in ICL to bypass IHX in case of a beam trip based on the feedback of the inlet and outlet temperatures of THX.

In the present study, the protected beam trip has the characteristics described in Figure 18. At the time of t=50 s, the beam power interrupt occurs. The duration of the beam switch-off is indicated as TBI. After then the beam power ramps up linearly in 20 seconds to full power again. The 3-way valve in ICL is switched to bypass IHX in 6 seconds after the beam trip starts, and kept closed for TVC seconds (to be defined in the simulations). The 3-way valve in SWL is regulated to an opening fraction of 0.14 toward SHX in 8 seconds after the beam trip begins and kept this position until 20 seconds after the 3-way valve in ICL starts to open.
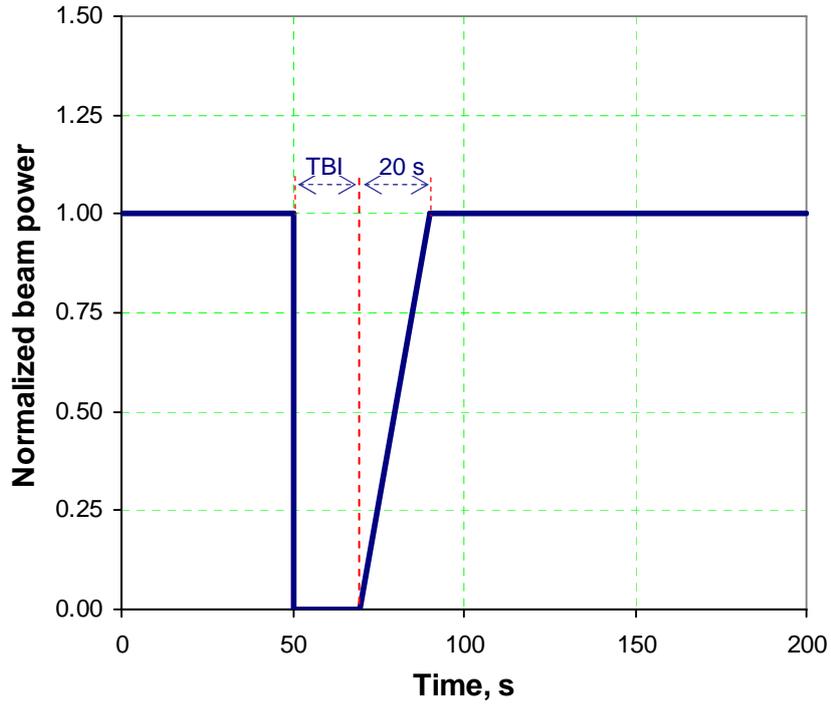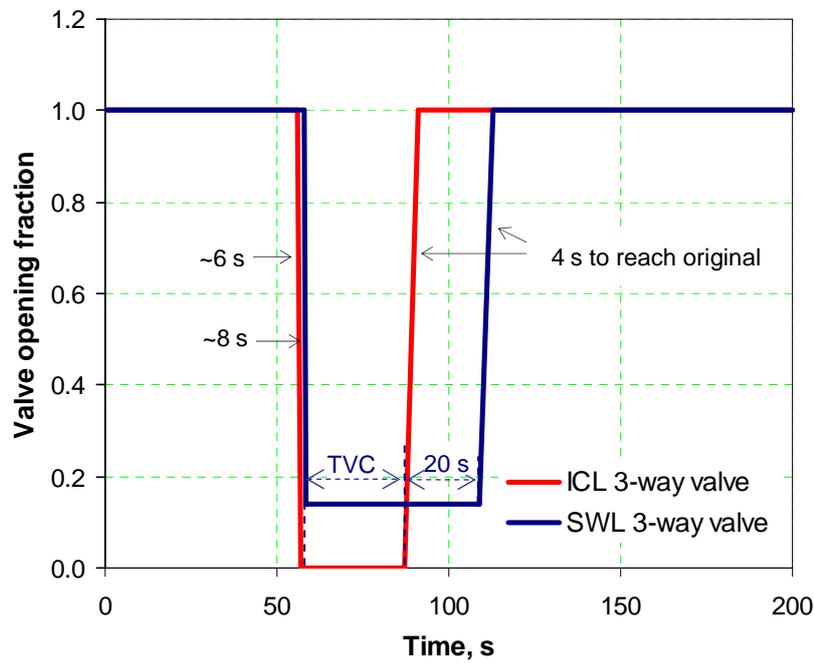
Figure 18 Simulation of the protected beam trip envisaged for the MEGAPIE operation. (a) Beam power as function of time; (b) Valve opening cross section as function of time.

For both ICL and SWL, the regulation of the 3-way valves is simulated by one valve at the inlet of the heat exchanger and another one at the bypass. The transient is simulated under the initial conditions of the MEGAPIE target, which are listed in Table 5.

Table 5: Initial conditions of the MEGAPIE target

Target thermal power deposition				581 kW		
Mass flow rate of main EMP				40.0 kg/s		
Mass flow rate of bypass EMP				2.5 kg/s		
	THX		IHX		SHX	
	Hot	Cold	Hot	Cold	Hot	Cold
Coolant	LBE	DTHT	DTHT	Water	Water	Water
Flow rate, kg/s	40.0	7.90	4.62	8.0	6.62	8.0
Inlet temperature, ^{o}C	326.6	146.9	175.9	52.8	70.4	30
Outlet temperature, ^{o}C	226.1	175.7	124.8	70.4	49.1	47.6

The heat sources other than the proton beam and the heat losses were taken into account in the simulations of MEGAPIE and MITS. For normal operation the additional heat sources are:

-- Main EMP: 7.770 kW,

-- Bypass EMP: 3.387 kW,

-- Oil pump in ICL: 20.6 kW,

-- Water pump in SWL: 16.7 kW;

and the heat losses:

-- Upper LMC: 1.443 kW,

-- Lower LMC: 4.121 kW,

-- Hot-leg of SWL: 1.140 kW,

-- Cold-leg of SWL: 0.513 kW.

Figure 19 shows the variations of temperatures at the THX inlet and exit of MEGAPIE for beam interrupt duration TBI of 3 s, 10 s and 20 s. For each case the LBE temperature at the THX inlet drops sharply after the beam interrupt due to the loss of heat source. It soon reaches its minimum and then rises quickly after the beam power is recovered. A temperature drop of about 70 ^{o}C – 95 ^{o}C is seen at the THX inlet. The LBE temperature at the THX

exit decreases after the beam trip starts, and increases when the beam power is recovered. Due to the delay of opening the 3-way valve in ICL, a small peak of fluid temperature is fore-seen at both the inlet and exit of THX after the beam power recovery. Because of the regulation of the 3-way valve in ICL, the temperature drop at the THX exit is much smaller than that of the LBE temperature at the THX inlet. It is expected that the longer the beam interrupt, the deeper the temperature drop. The present study shows the effectiveness of the regulation of the 3-way valve to limit large LBE temperature fluctuation at the exit of THX under the beam trip transient.
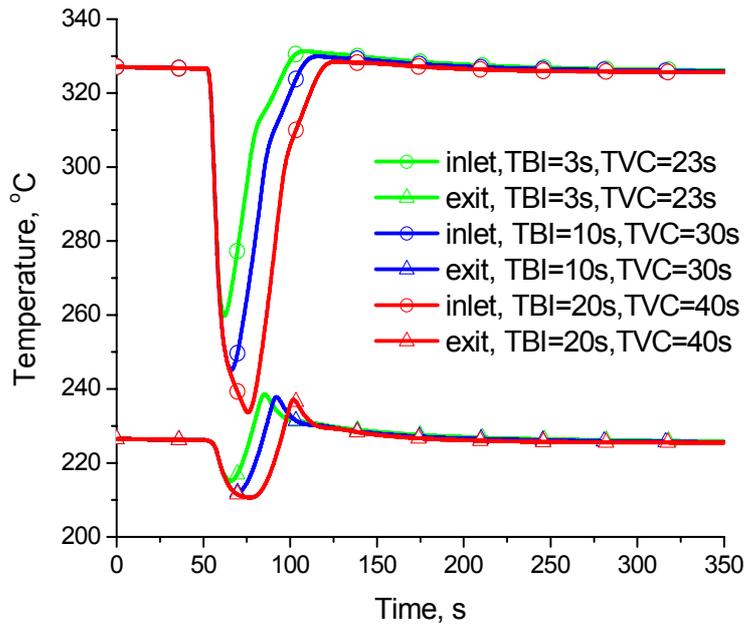

Figure 19 Variation of THX inlet and exit LBE temperatures for different
beam interrupts of MEGAPIE

Variations of temperatures at the THX inlet and exit of MEGAPIE for different values of TVC are shown in Figure 20. It is seen that the peaks of LBE temperatures at the THX inlet and exit after the beam power recovery can be reduced by opening the 3-way valve in ICL earlier. For beam interrupt of 10 s, the peaks of LBE temperatures at the inlet and exit of THX are eliminated when the 3-way valve in ICL is opened 10 s after the beam power recovery begins, i.e. TVC = 20 s.

The behavior of LBE temperature under protected beam trip was investigated for MITS under the initial conditions listed in Table 6. As shown in Figure 21, the temperature trend under protected beam trip of MITS is similar to that of the MEGAPIE. However, the drop of the fluid temperature of MITS under protected beam trip is much smaller than that of MEGAPIE.

In Figure 22, a comparison of the LBE temperature drop in the THX of MITS simulated by ATHLET-MF with that calculated by Equation (14) for the protected beam trip is given. It is seen that, during the transient of beam trip, the discrepancy is remarkable between the tem-

perature drop in the THX of MITS and that calculated by Equation (14) on the basis of the temperature drop of MEGAPIE. The discrepancy of fluid temperature between MEGAPIE and MITS under transient conditions is expected since the heat transfer from the target system to the intermediate cooling loop, and from the intermediate cooling loop to the secondary water loop, and the total mass of the structure were not scaled by the proposed relationships.
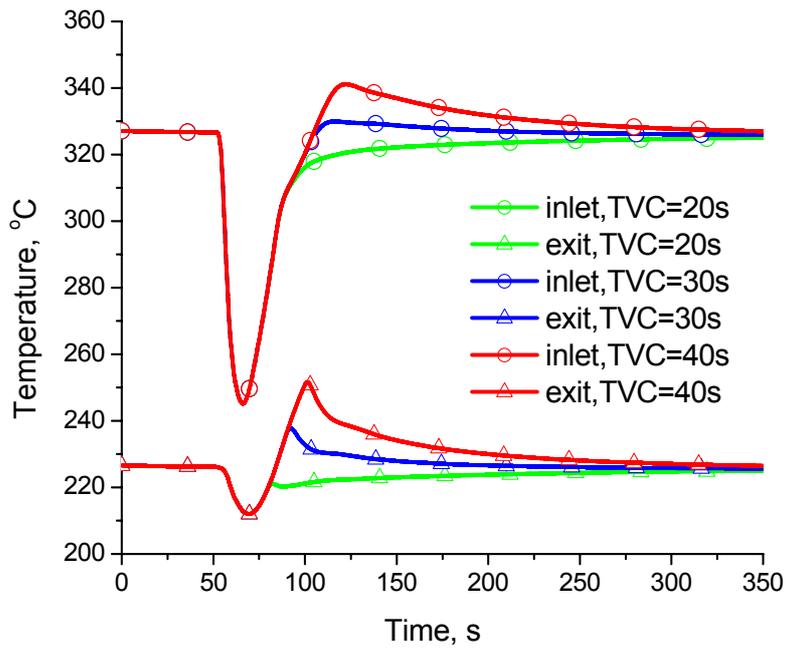
Figure 20 Variation of THX inlet and exit LBE temperatures of MEGAPIE
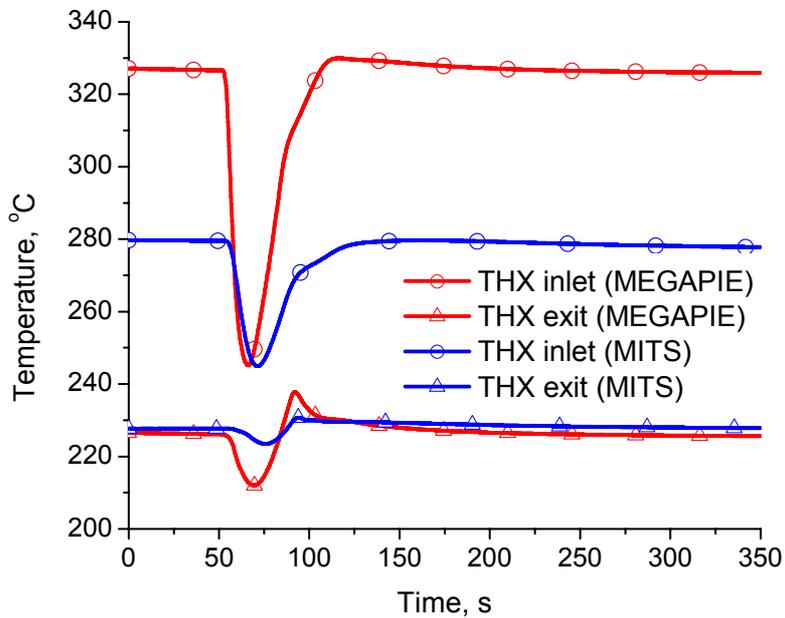for different closed times of ICL 3-way valve (TBI=10 s)

Figure 21 Comparison of THX inlet and exit LBE temperatures under
beam interrupt (TBI=10 s, TVC=30 s)

Table 6: Initial Conditions of MITS

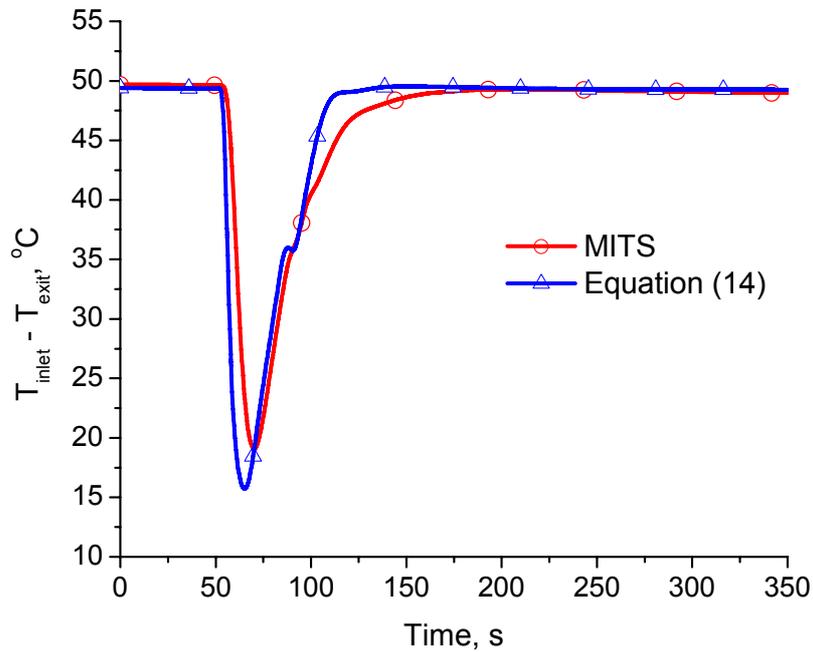|			THX		IHX		SHX	
Target thermal power deposition		200 kW						
Mass flow rate of main EMP		28.0 kg/s						
Mass flow rate of bypass EMP		1.75 kg/s						
		THX		IHX		SHX		
		Hot	Cold	Hot	Cold	Hot	Cold	
Coolant		LBE	DTHT	DTHT	Water	Water	Water	
Flow rate, kg/s		28.0	5.54	3.233	5.57	4.60	5.61	
Inlet temperature, $^{\circ}$C		279.5	183.2	197.3	88.2	97.5	30	
Outlet temperature, $^{\circ}$C		229.9	197.0	172.8	97.5	86.2	39.3	

Figure 22 Variation of LBE temperature drop in the THX of MITS
under beam interrupt (TBI=10 s, TVC=30 s)

36

3.2.3 Transients of loss of pump head

The simulations of the natural circulation of liquid LBE of MEGAPIE and MITS were carried out by assuming that both the main EMP and the bypass EMP are turned off at the normal target operational conditions without beam trip. The decay flow rates of the main EMP and bypass EMP after power supply off are listed in Table 7.

Table 7: Normalized LBE decay flow after power supply off

time, s	Main EMP	time, s	Main EMP
0	1	30	0.459
6	0.956	40	0.312
10	0.918	46	0.224
15	0.809	54	0.142
20	0.694	66	0.077
25	0.585	75	0.0
time, s	Bypass EMP	time, s	Bypass EMP
0	1.0	12	0.253
2	0.950	15	0.135
4	0.852	18	0.059
6	0.674	21	0.011
8	0.512	22	0.0
10	0.372		

Figure 23 shows the normalized LBE mass flow rate after the loss of pump power supply. It is seen that the steady state natural circulation of LBE with a mass flow rate of about 46% of initial flow for MEGAPIE and of about 37% of initial flow for MITS is established soon after the end of the phase of decay flow. The flow rate of natural circulation of MITS is about 24% less than that calculated by Equation (14) on the basis of the flow rate of natural circulation of MEGAPIE. As shown in Figure 24, the LBE temperature at the inlet of THX increases and the LBE temperature at the exit of THX decreases after the two pumps are turned off due to the reduction of LBE flow rate. The beam window temperature and its integrity under the loss of pump power supply will be assessed by a numerical simulation using a CFD code.
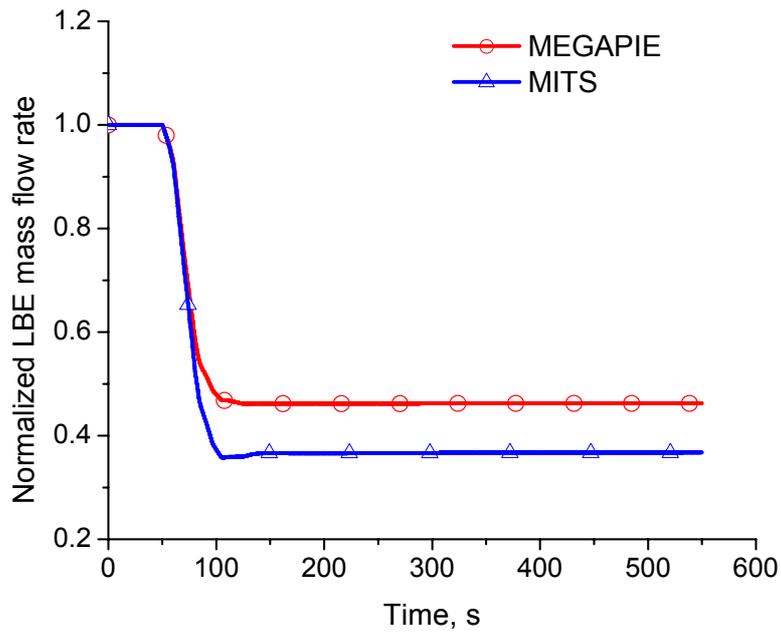
Figure 23 Normalized LBE mass flow rate for a pump loss in the
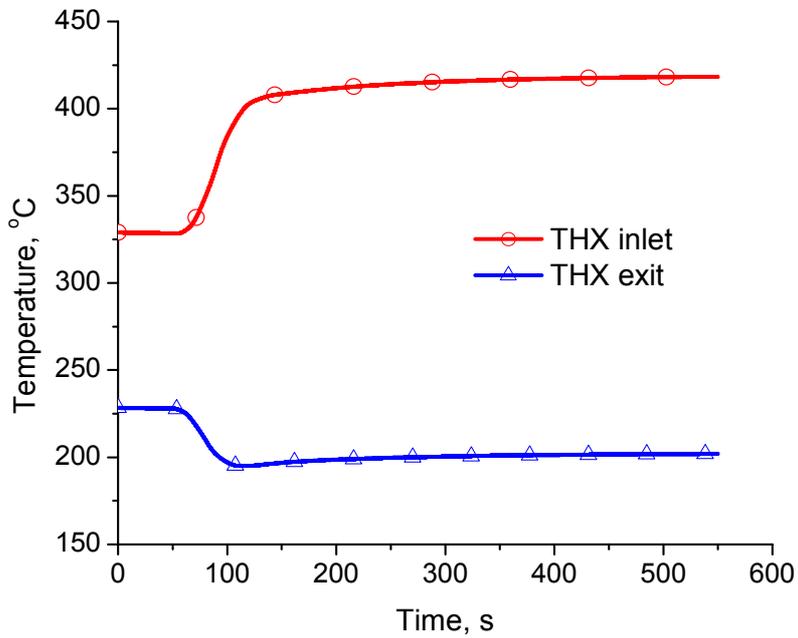MEGAPIE and in the MITS

Figure 24 Variation of THX inlet and exit LBE temperatures for a
total pump loss in the MEGAPIE target

4 SUMMARY

A new version of ATHLET has been developed for the thermal-hydraulic analysis of multi-fluid systems, including the liquid LBE-cooled systems. Fluid indexes were introduced in the new code ATHLET-MF, and the code was modified in such a way that a user can easily adapt the code for various fluids.

A set of empirical equations of the properties of liquid LBE were proposed for use in ATHLET-MF based on a comprehensive review and assessment on the available data and equations of the thermophysical properties of liquid LBE in open literature. These recommended equations of the LBE thermophysical properties were implemented into the ATHLET-MF code. Equations of DTHT properties and single phase convective heat transfer correlation of liquid LBE were also implemented in ATHLET-MF.

The ATHLET-MF code was assessed against HERETA and HETRAF by performing the simulation of the dynamic behavior of the target cooling system of XADS under beam power switch-on conditions. Comparison of ATHLET-MF with two other system analysis codes confirms the applicability of the ATHLET-MF code to LBE cooled systems.

Transients of beam power switch-on, loss of heat sink and beam trip were simulated with ATHLET-MF for the target cooling system of XADS. A beam power switch-on causes a sharp increase in the fluid temperature and a high temperature peak. The integrity of the beam window under such conditions needs to be checked. Loss of heat sink results in an increase in fluid temperature and a decrease in mass flow rate. To avoid the damage of the target, the proton beam should be switched off in 200 s after the occurrence of the transient.

The regulation of the 3-way valve in ICL can effectively limit the LBE temperature fluctuation at the THX exit of MEGAPIE and of MITS under beam interrupt conditions. The peaks of LBE temperatures at the THX inlet and exit after the beam power recovery can be reduced or even eliminated by opening the 3-way valve in ICL at an early time.

The MITS shows similar system thermalhydraulic behavior as that of the MEGAPIE for the protected beam trip. However, the drop of fluid temperature under the transient of beam trip of MITS is much smaller than that of the MEGAPIE. The steady state natural circulation of LBE is established shortly after the loss of pump power supply for both MEGAPIE and MITS. The natural circulation flow rate is about 46% of initial flow for MEGAPIE, and of about 37% of initial flow for MITS.

The present study shows that the application of the proposed scaling principles for flow rate and temperature of the integral test will cause a remarkable deviation between the MEGAPIE and the scaled experiment.

Future efforts will be made for the assessment of the ATHLET-MF code by using experimental data.

ACKNOWLEDGMENTS

REFERENCES

Alchagirov, B.B. et al., 2003, Experimental investigation of the density of molten Lead-Bismuth eutectic. High Temperature, 41, 247‑253.

Austregesilo, H. et al., 2000, ATHLET Mod1.2 Cycle --- models and methods. Gesellschaft für Anlagen- und Reaktorsicherheit mbh, Garching.

Bauer, G. S., Salvatores, M., Heusener, G., 2001, MEGAPIE, a 1 MW pilot experiment for a liquid metal spallation target. Proc. of the 4th Internat. Workshop on Spallaton Materials Technology (IWSMT-4), Schruns, A, October 8-13, 2000, Journal of Nuclear Materials, 296, 17-33.

Bienias, A., Sauerwald, F., 1927, Die innere Reibung von Kupfer, antimon, Blei und Kupfer-Antimon-, Kupfer-Zinn-, Blei-Wismut-Legierungen, Z. Anorg. U. allg. Chem. 93, 51-75.

Buono, S. et al., 1997, Main properties of Lead. CERN/ET/Internal Note 97-07.

Cevolani, S., 1998, Review of the liquid lead-bismuth alloy physical properties. ENEA Casaccia Technical Note, SIEC/DT/SDB.00004.

Cheng, X., 1994, Numerical analysis of thermally induced transients in forced flow of super-critical helium. Cryogenics, **34**, 195-201.

Cheng, X., Slessarev, I., 2000, Thermal-hydraulic investigations on liquid metal target systems. J. Nuclear Engineering and Design, **202**, 297-310.

Cheng, X., Pettan, C., Knebel, J. U., Chen, H.Y., 2002, Experimental studies supporting the design of a 1 MW LEB target. Proceedings of seventh information exchange meeting on actinide and fission product partitioning and transmutation. Jeju, Republic of Korea, October 14-16, 2002, CD-ROM 595-604, Paris : OECD/NEA, 2003.

Cheng, X., Neitzel, H. J., Batta, A, Knebel, J. U., Coors, D. Vanvor, D., Freudenstein, K., 2003, Design Analysis of the spallation target for the European Experimental ADS. AccApp'03 : Accelerator Applications in a Nuclear Renaissance, San Diego, Calif., June 1-5, 2003.

Cheng, X., Batta, A., Chen, H .Y., Tak, N. I., 2004, Turbulent heat transfer to heavy liquid metals in circular tubes, ASME Heat Transfer and Fluids Engineering Summer Conference: Charlotte, N. C., July 11-15, 2004, HT-FED2004-56562

Cinotti, L., 2001a, XADS Pb-Bi cooled experimental accelerator driven system – reference configuration – summary report. Ansaldo ADS1SIFX0500, Ansaldo Nucleare, Genova, Italy.

Cinotti, L., 2001b, Conception and development of a Pb-Bi cooled experimental ADS. ANS winter meeting, Reno, USA, November 12-15, 2001.

Davis, C. B., Shieh, A. S., 2000, Overview of the use of ATHENA for thermal-hydraulic analysis of systems with Lead-Bismuth coolant. 8th international conference on nuclear engineering. Baltimore, MD USA, April 2-6, 2001.

Department of Energy, A Roadmap for Developing Accelerator Transmutation of Waste (ATW) Technology: A Report to Congress. October 1999, DOE/RW-0519. http://www.pnl.gov/ATW/ReportToCongress/

Dwyer, O.E., 1996, Recent development in liquid metal heat transfer, *Atomic Energy Review*, 4, No.1.

ENEA, 2001, A European roadmap for developing accelerator driven systems (ADS) for nuclear waste incineration, ENEA, Roma.

Friedland, A.J., 1966. Coolant properties, heat transfer and fluid flow of liquid metals. Fast Reactor Technology: Plant Design, J.G. Yevick, Ed., Chapt.2, The M.I.T. Press, Cambridge, USA.

GRS. 2001. ATHLET User's Manual.

Holman, J.P. 1968. HEAT TRANSFER. MacGraw-Hill, USA.

Hultgren, R. et al. 1973. Selected Values of the Thermodynamic Properties of the Elements. American Soc. of Metals, Metals Park, Ohio, USA.

Iida, T., Guthrie, R. I. 1988. The Physical Properties of Liquid Metals. Clarendon Press, Oxford, UK.

Imbeni, V. et al. 1999. Properties of the eutectic alloys Pb55.5Bi and Pb17Li. Institute of Metallurgy, University of Bologna, Italy.

INSC – The International Nuclear Safety Center of Argonne National Laboratory, http://www.insc.anl.gov/.

Knebel, J. U. 2002. Overview of the P & T activities at Forschungszentrum Karlsruhe. Proceedings of seventh information exchange meeting on actinide and fission product partitioning and transmutation. Jeju, Republic of Korea, October 14-16, 2002, Proc. on CD-ROM, pp. 139-159, Paris : OECD/NEA, 2003.

Knebel, J. U., Cheng, X., Tak, N. I. 2001. Thermalhydraulic design of the MEGAPIE spallation target. 5th Topical Meeting on Nuclear Applications of Accelerator Technology, Reno, USA, November 11-15, 2001.

Kutateladze, S. S. et al. 1959. Liquid metal heat transfer media. Chapman & Hall, Ltd. London.

Leung, W. H., Sigg, B. 2003. unpublished report.

Lyon, R.N. 1952. Liquid metals handbook. Report NAVEXOS P-733, U.S. Government Printing Office, Washington, D.C., USA.

MacLain, S., Martens, J. H. 1964. Reactor Handbook. Volume IV. Interscience Publ., John Wiley & Sons.

Morita, K., Maschek, W., Flad, M. 2004. Thermophysical properties of Lead-Bismuth eutectic alloy for use in reactor safety analysis. 2nd Meeting of NEA Nuclear Science Committee Working Group on LBE Technology of the Working Party on Scientific Issues of the Fuel Cycle (WPFC), Issy-les-Moulineaux, France,, September 23-24, 2004.

Mukaiyama, T. et al. 1997. Omega Program & Neutron Science Project for Developing Accelerator Hybrid System at JAERI, Proceedings of the I.A.E.A. Technical Committee Meeting on: Feasibility and Motivation for Hybrid Concepts for Nuclear Energy Generation and Transmutation, Madrid, Spain, September 17-19, 1997, IAEA-TC-903.3, pp. 179-194.

Neitzel, H. J., Knebel, J. U. 2002. Auslegung eines geschlossenen 4 MW-Targetmoduls mit Wärmeabfuhrsystem für eine ADS-Anordnung. Wissenschaftliche Berichte FZKA 6687, Forschungszentrum Karlsruhe.

Neitzel, H. J., 2003. private communication.

Petrazzini, M. 2002. Lead Bismuth Eutectic Physical Properties and Thermodynamic Tables. Ansaldo Nucleare, Genova, Italy.

Richard, P. 2002. Technical Specifications, Missions of XADS, Recommendations for the Main Characteristics. DER/SERI/LCSI-02/4002, CEA, France.

Rubbia, C. 1995. Conceptual design of a fast neutron operated high power energy amplifier. CERN/AT/95-44.

Sobolev, V. 2002. Database of thermal properties for the melted Lead-Bismuth Eutectic. RF&M Dept. SCK·CEN, Belgium.

Tak, N., Neitzel, H.J., Cheng, X. 2005. Computational fluid dynamics analysis of spallation target for experimental accelerator-driven transmutation system, *Nuclear Engineering and Design*, Vol. 235, pp.761-772.

Touloukian, V.I. et al. 1970. Thermophysical properties of matter. Thermal conductivity of metallic liquids. IFI/Plenum, New York.

Young, D. A. 1977. A soft-sphere model for liquid metals. Lawrence Livermore Laboratory, USA